Article

Unlocking Nicotinic Selectivity via Direct C–H Functionalization of (−)-Cytisine

Hugo Rego Campello, Silvia G. Del Villar, Aurélien Honraedt, ..., Adrian J. Mulholland, Susan Wonnacott, Timothy Gallagher

t.gallagher@bristol.ac.uk

HIGHLIGHTS

Efficient and highly flexible C(10) functionalization of (−)-cytisine

Ligands with enhanced selectivity for α4β2 nicotinic acetylcholine receptor subtypes

Reduced affinity and loss of agonist profile at α7

Receptor features that link to subtype selectivity are identified

Efficient access to C(10) of (−)-cytisine via C–H activation provides access to enantiomerically pure nicotinic acetylcholine receptor ligands that target the high-affinity nicotine α4β2 subtype with enhanced selectivity. These C(10) cytisine variants retain a partial agonist profile at the α4β2 subtype but, critically, display negligible activity at the α7 receptor subtype. Using computational methods, Gallagher and colleagues link receptor selectivity to key protein residues associated with, as well as beyond, the immediate ligand binding site.

Chem

Article

Unlocking Nicotinic Selectivity via Direct C–H Functionalization of (−)-Cytisine

Hugo Rego Campello,[1] Silvia G. Del Villar,[2] Aurélien Honraedt,[1] Teresa Minguez,[2] A. Sofia F. Oliveira,[1,3] Kara E. Ranaghan,[1] Deborah K. Shoemark,[3] Isabel Bermudez,[2] Cecilia Gotti,[4] Richard B. Sessions,[3] Adrian J. Mulholland,[1] Susan Wonnacott,[5] and Timothy Gallagher[1,6,*]

SUMMARY

Differentiating nicotinic acetylcholine receptors (nAChR) to target the high-affinity nicotine α4β2 subtype is a major challenge in developing effective addiction therapies. Although cytisine 1 and varenicline 2 (current smoking-cessation agents) are partial agonists of α4β2, these drugs display full agonism at the α7 nAChR subtype. Site-specific modification of (−)-cytisine via Ir-catalyzed C–H activation provides access to C(10) variants 6–10, 13, 14, 17, 20, and 22, and docking studies reveal that C(10) substitution targets the complementary region of the receptor binding site, mediating subtype differentiation. C(10)-modified cytisine ligands retain affinity for α4β2 nAChR and are partial agonists, show enhanced selectivity for α4β2 versus both α3β4 and α7 subtypes, and critically, display negligible activity at α7. Molecular dynamics simulations link the C(10) moiety to receptor subtype differentiation; key residues beyond the immediate binding site are identified, and molecular-level conformational behavior responsible for these crucial differences is characterized.

INTRODUCTION

Validated links exist between neuronal nicotinic acetylcholine receptors (nAChR)[1–4] and a range of neurodegenerative[5] and psychiatric diseases.[6] Interest in these conditions, together with the broader public health issue of tobacco consumption and addiction,[7,8] a global challenge highlighted by the landmark World Health Organization Framework Convention on Tobacco Control,[9] has driven the discovery and evaluation of small molecule ligands for therapeutic intervention, notably for smoking cessation.[10,11] These molecules are often derived from natural product leads, such as nicotine, but a continuing goal is to identify ligands with higher selectivity for targeting nAChR subtypes such as α4β2 (the prime receptor for smoked nicotine because of its high-affinity nicotine binding sites) coupled with sufficient bioavailability to enable central nervous system penetration.[12,13]

Our activity in this area is focused on (−)-cytisine 1 (Figure 1).[14] Currently marketed for smoking cessation as Tabex, (−)-cytisine, which is isolated from *Cytisus laburnum* (Golden Rain acacia), has been used in eastern Europe for well over 50 years.[15,16] The partial agonist profile of 1 at α4β2 nAChR differentiates this natural product from full agonists, such as acetylcholine. Two recent controlled clinical trials have reported[17,18] further support for the effectiveness of cytisine 1 for smoking cessation. Cytisine, which is more effective than nicotine replacement therapy, offers the potential of a readily available and efficacious, as well as cost-effective, smoking-cessation protocol.[19] A synthetic variant, varenicline 2 (launched in 2006 as Champix and Chantix; Figure 1)[20–23] offers a broadly comparable profile with that of 1 for α4β2

The Bigger Picture

Molecular locksmithing is the use of precision chemical keys for biological locks. Nicotinic acetylcholine receptors (nAChR) associated with acetylcholine neurotransmission are linked to public health issues, notably tobacco addiction. Why is this important? Smoking kills seven million people annually and imposes a huge burden in terms of healthcare and lost productivity. The ability to design a molecule to achieve high receptor selectivity is paramount for the success of smoking cessation: poor selectivity is typically accompanied by (adverse) side effects. We have modified cytisine, a known "nicotinic activator," in a very direct and versatile manner to suppress a particular characteristic: activation of the α7 subtype of nAChR. Computational molecular simulation of the protein-ligand complexes links these structural changes to a ligand's activity, facilitating the design of precision "molecular keys" for better discrimination of receptor subtypes and offering the potential of more targeted therapies.
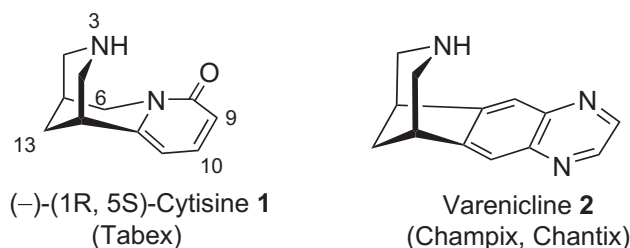
Figure 1. Cytisine 1 and Varenicline 2, Nicotinic Partial Agonists at α4β2 nAChR, and Full Agonists at α7 nAChR

nAChR, and these commercial products have led to partial agonism being regarded as a key feature for successful intervention to combat nicotine addiction.[10] However, both cytisine[24] and varenicline[25] are also full agonists (*in vitro*) at the α7 (where varenicline **2** is more potent than cytisine **1**[26]) and α3β4 nAChR subtypes, albeit with differing potencies, but nevertheless contributing to the potential of off-target side effects. A contemporary goal, therefore, is to develop partial agonists for the α4β2 nAChR with enhanced nAChR subtype selectivity.

The biological target, the two agonist binding sites of α4β2 nAChR, is located at the interface of α and β subunits of this pentameric receptor.[1,2] The α subunit contributes the primary component comprising key aromatic amino acids and the highly conserved C loop. This accommodates (protonated) N(3) of **1** via an interplay of cation-π and hydrogen-bonding interactions[27–29] and is an interaction that is highly sensitive to structural modification in this region of the ligand.[30] The pyridone moiety of **1**, however, binds within the complementary region of the site provided by the adjacent β subunit (or the opposite face of an α7 subunit in the homomeric α7 nAChR). This region influences subtype selectivity for agonists, and in the case of cytisine, higher selectivity for the α4β2 nAChR subtype over α3β4 is associated with substitution at C(10).[31–33] For example, relative to cytisine **1** (which is 150-fold more selective at α4β2 than α3β4), the C(10) methyl analog (racemic variant of **10** below) shows a 3,500-fold selectivity in binding affinity for the α4β2 (relative to α3β4) nAChR subtype.[32] This provides an impetus to explore modification of the pyridone moiety of **1** as an attractive avenue for further enhancing nAChR subtype selectivity. However, previous access to C(10) substituted cytisine ligands has required lengthy synthetic sequences (at least ten chemical steps) limiting both the number and variety of C(10) options available. Moreover, only racemic ligands have been reported to date;[31–33] although the (+)-enantiomer ((+)-**1**) lacks a nicotinic profile,[34] the broader characteristics (e.g., toxicology) of (+)-**1** remain unclear, highlighting the value of targeting enantiomerically pure variants. Accordingly, there is a significant hurdle to overcome: given the inherent bias of the pyridone moiety for electrophilic substitution at C(9) and C(11), how do we specifically target C(10) of (−)-cytisine **1** directly, efficiently, and with the ability to access a wide range of structural variation?

RESULTS

Synthesis of (−)-Cytisine C(10) Variants

Here we demonstrate how to manipulate directly (−)-cytisine **1** at C(10) in a highly versatile manner. This chemistry leads efficiently and flexibly to cytisine variants with (1) enhanced α4β2 selectivity (versus both α3β4 and α7) that retain the essential partial agonist profile suited to smoking cessation, and (2) that also show a negligible agonist profile for α7 nAChR. Functionalization of (−)-**1** has been achieved by highly efficient Ir-catalyzed borylation within the pyridone moiety[35] of cytisine. This C–H activation process occurs exclusively at C(10) within the pyridone ring

[1]School of Chemistry, University of Bristol, Bristol BS8 1TS, UK

[2]Department of Biological and Medical Sciences, Oxford Brookes University, Oxford OX3 0BP, UK
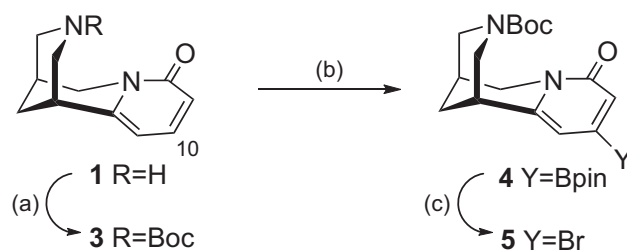
[3]School of Biochemistry, University of Bristol, Bristol BS8 1TD, UK

[4]CNR, Institute of Neuroscience, Biometra Department, University of Milan, Milan 20129, Italy

[5]Department of Biology and Biochemistry, University of Bath, Bath BA2 7AY, UK

[6]Lead Contact

*Correspondence: t.gallagher@bristol.ac.uk

https://doi.org/10.1016/j.chempr.2018.05.007

Scheme 1. Ir-Catalyzed C(10) Borylation of N-Boc cytisine 3
Reagents and reactions conditions were as follows: (a) Boc$_2$O, Na$_2$CO$_3$, THF, H$_2$O (93%);
(b) [Ir(COD)(OMe)]$_2$ (1 mol %), dtbpy (2 mol %), B$_2$pin$_2$ (0.70 equiv), THF (0.7 M with respect to **3**),
reflux (100% conversion by ^{1}H NMR); (c) CuBr$_2$ (3 equiv), MeOH, H$_2$O, air (83%). Abbreviations: Boc,
CO$_2t$-Bu; B$_2$pin$_2$, bis(pinacolato)diboron; dtbpy, 4,4'-di-tert-butyl-2,2'-dipyridyl; Me4phen, 3,4,7,8-
tetramethyl-1,10-phenanthroline; THF, tetrahydrofuran.

(Scheme 1) and the functionality introduced (i.e., the C(10) boronate ester **4** or
derived bromide **5**) provides essentially unfettered means of varying the C(10)
substituent. A significant consequence of this chemistry is that all resulting C(10)
ligands produced are single enantiomers.

Ir-catalyzed C–H activation and C(10) site-specific borylation can be conducted with
(−)-cytisine **1** itself but in our hands this required an excess (1.5–3.0 equiv) of B$_2$pin$_2$
and the instability of the resulting 10-(Bpin)cytisine proved to be a limitation. N-Boc
cytisine **3** (available in high yield from (−)-cytisine **1**) provides, however, an optimal
substrate, offering excellent chemical efficiency and conversion (only 0.70 equiv of
B$_2$pin$_2$ needed), very good product stability, and easy scale-up: borylation of **3** to
give **4** has been done on a 5-g scale (with 0.6 mol % of [Ir(COD)(OMe)]$_2$). No purifi-
cation was required and crude **4** was used directly as illustrated by conversion to bro-
mide **5** (in 77% overall yield over three steps) from (−)-**1** (Scheme 1). Further and
importantly, this chemistry offers significant flexibility in terms of the scope of down-
stream processing options and the range of C(10) cytisine variants that are available.

Intermediates **4** and **5** offer highly complementary synthetic options for exploring a
comprehensive structure-activity profile for the α4β2 nAChR by using enantiomeri-
cally pure cytisine-based ligands that are easily isolated and purified. Here, we
present a representative selection of these C(10) ligands together with preliminary
biological data: binding affinity and functional potency (agonist potency and effi-
cacy) profiles that demonstrate nAChR subtype selectivity. These data, combined
with molecular modeling and simulation, allow us to propose a rationale for the
subtype selectivity profiles we have observed.

Exploiting the reactivity profiles of both **4** and **5** is illustrated in Scheme 2. Use of the
crude 10-borylated adduct **4** via direct oxidation or copper-catalyzed Chan-Lam
coupling led to the 10-hydroxy and 10-methoxycytisine derivatives **6** and **7**, respec-
tively, after N-Boc cleavage (**4**) or inverse sense (via **5**), provided the 10-arylated
adducts **8** and **9**. Chemistry using **4** has also been exploited to introduce other
heteroatom-based substituents at C(10) as well as a wide range of other 10-aryl
and heteroaryl variants, and full details of this will be reported in due course.

The 10-bromo derivative **5** also enables a variety of C–C bond-forming processes to be
exploited. Although Stille-type coupling using Me$_4$Sn provided the 10-methyl derivative
10 in essentially quantitative yield, toxic alkyltins are avoidable, and **10** was also available
in (an unoptimized) 64% yield from boronate ester **4** via Pd-catalyzed methylation
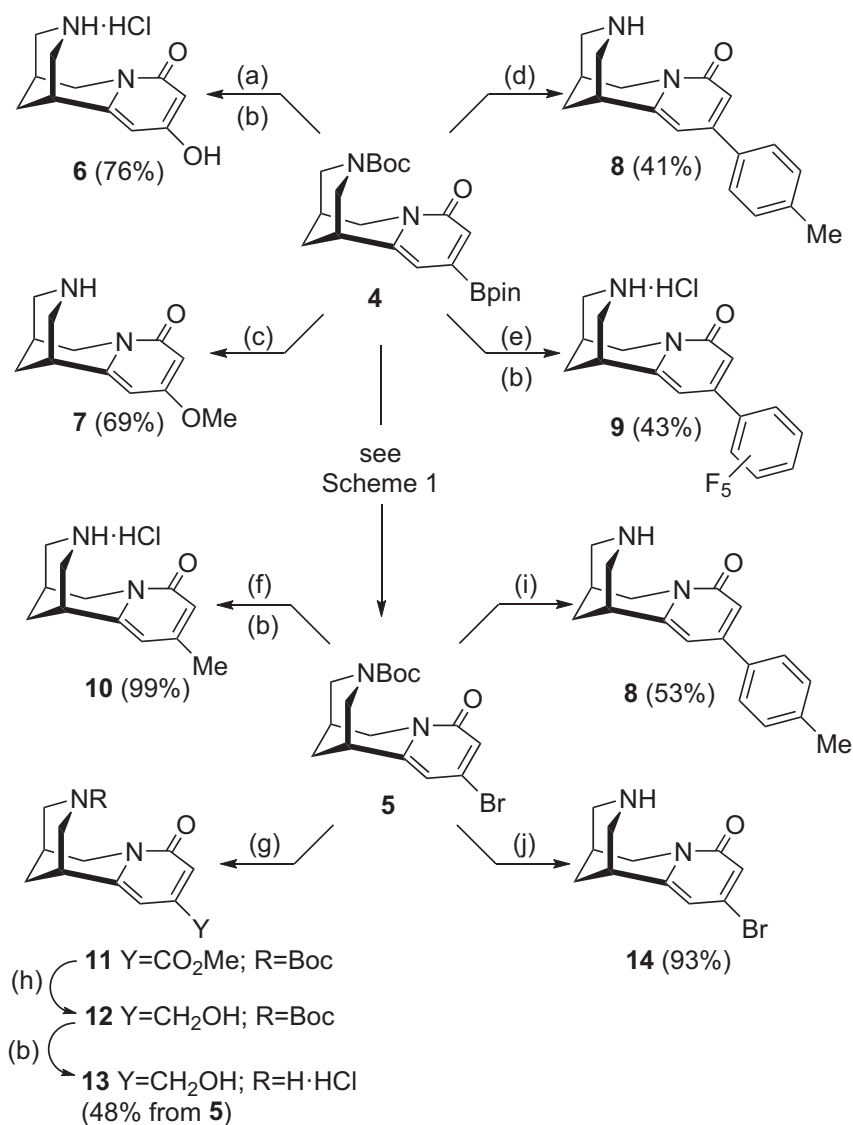
Scheme 2. Transformations Based on 4 and 5 to Provide C(10)-Substituted Cytisine Ligands

Yields shown below are for transformations other than (b), i.e., N-Boc cleavage. This step was common to all examples except for **7**, **8**, and **14** (where trifluoroacetic acid [TFA] and dichloromethane [DCM] were used), and overall isolated yields (i.e., including b, where appropriate) are shown under the product structure. Final products were isolated as HCl salts except for **7**, **8**, and **14**, which were isolated as free bases. Reagents and reactions conditions were as follows: (a) 30% aqueous H_2O_2, NaOH, room temperature (RT) (79%); (b) HCl in MeOH, RT; (c) (1) $CuSO_4$, MeOH, KOH, MS 4Å, O_2 (balloon), 65°C; (2) TFA, DCM, RT (69% overall); (d) (1) 4-BrC$_6$H$_4$Me, Pd(PPh$_3$)$_4$, K_2CO_3, DME/H$_2$O, 80°C; (2) TFA, DCM, RT (41% overall); (e) BrC$_6$F$_5$, PdCl$_2$(PPh$_3$)$_2$, Cs$_2$CO$_3$, THF, reflux (99%); (f) Me$_4$Sn, PdCl$_2$(PPh$_3$)$_2$, PhMe, 100°C (99%); ligand **10** is also available from **4** via Pd-catalyzed methylation (see main text and Supplemental Information); (g) Pd(OAc)$_2$, dppp, Et$_3$N, DMF, MeOH, CO, 80°C (86%); (h) LiAlH$_4$, THF, −78°C (62%); (i) (1) 4MeC$_6$H$_4$B(OH)$_2$, Pd(PPh$_3$)$_4$, K_2CO_3, DME/H$_2$O, 80°C; (2) TFA, DCM, RT (53% overall); (j) TFA, DCM, RT (93%). Abbreviations: DCM, dichloromethane; DME, dimethoxyethane; dppp, bis(diphenylphosphino) propane; TFA, trifluoroacetic acid.

involving MeI. Pd-catalyzed carbonylation of **5** gave ester **11**, reduction of which gave **12**, and subsequent Boc deprotection generated 10-(hydroxymethyl)cytisine **13**; both **10** and **13** have previously been prepared by Kozikowski and co-workers[31,32] but only
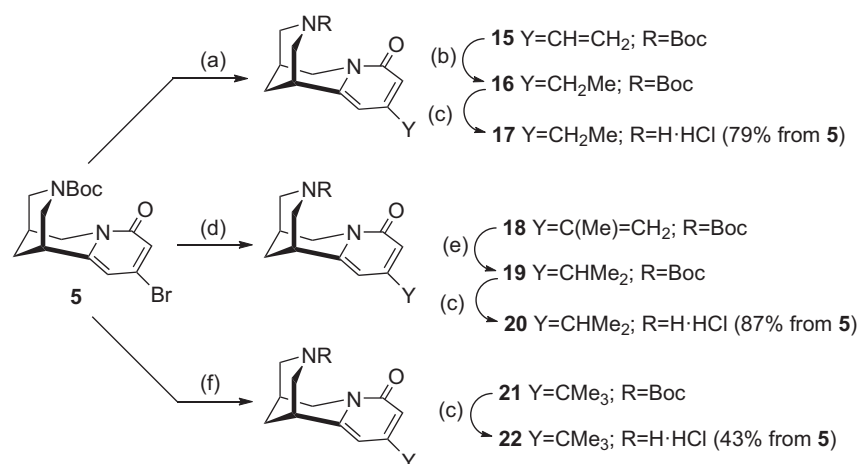
Scheme 3. C(10)-Alkyl Variation of Cytisine

Yields shown below are for transformations other than (c), i.e., N-Boc cleavage. This step was common to all examples, and overall isolated yields (i.e., including c) are shown under the product structure. Final products were isolated as HCl salts. Reagents and reactions conditions were as follows: (a) $(CH_2=CHBO)_3 \cdot py$, K_2CO_3, $PdCl_2(PPh_3)_2$, dioxane, water, 90°C (86%); (b) Pd/C, H_2, MeOH (95%); (c) HCl in MeOH, RT; (d) $CH_2=C(Me)Bpin$, $NaHCO_3$, $Pd(PPh_3)_4$, water, dioxane, 60°C (94%); (e) $TolSO_2NHNH_2$, K_2CO_3, MeCN, reflux (95%); (f) Me_3CMgCl, CuI, THF, −40°C (42%).

as racemates and with lengthy sequences (at least ten steps). Bromide **5** is also effective in Suzuki-Miyaura cross-coupling in that it offers an alternative entry to **8**. Finally, 10-halo variants were of interest, and for that reason, 10-bromocytisine **14** was prepared. The development of more focused structural libraries, guided by the biological profiles associated with C(10) substituted cytisine leads, is also now fully enabled by ready availability on scale of both **4** and **5**. This, in turn, underscores the value of being able to achieve the direct, 100% regioselective, and highly efficient C–H functionalization of N-Boc cytisine **3** (shown in Scheme 1).

Probing Subtype Selectivity as a Function of C(10) Alkyl Variation

The level of subtype differentiation (compared with cytisine **1**) observed for 10-methylcytisine **10** (see below) prompted us, by way of exemplification, to explore one focused library by varying the C(10) alkyl residue. This largely limits changes to bulk and lipophilicity, and with the flexibility associated with the reactivity of bromide **5**, the C(10) ethyl, *iso*-propyl, and *tert*-butyl variants **17**, **20**, and **22** were synthesized (Scheme 3). A Suzuki-Miyaura cross-coupling approach enabled access to the 10-ethenyl adduct **15**, and alkene reduction of this followed by Boc cleavage of **16** gave the 10-ethyl cytisine variant **17**. An analogous cross-coupling provided the isopropenyl adduct **18**, which was reduced to give **19** and deprotected to provide **20**. Direct introduction of a *tert*-butyl moiety is achievable with a copper catalyst under the Kumada-Corriu-Tamao reaction developed by Hintermann et al.[36] This chemistry, which was developed with haloazines and diazines, had not been applied previously to 2-pyridones but is effective in providing adduct **21**. Deprotection then afforded **22**, completing a homologous series of ligands from cytisine **1** (H at C(10)) to **22** (*tert*-Bu at C(10)).

In Vitro Biological Evaluation

Binding Affinities

Two sets of biological data establish the superior selectivity of the ligands shown in Schemes 2 and 3 for human α4β2 nAChR, supporting their potential as candidates for smoking cessation. Binding-affinity profiles across three human nAChR subtypes

Table 1. Affinity (K_i in nM) of C(10) Ligands for α4β2, α3β4, and α7 nAChR Subtypes

Ligand	α4β2[a]	α3β4[a]	α7[a]	α3β4/α4β2	α7/α4β2
	K_i	K_i	K_i		
(−)-Cytisine **1**	1.27 ± 0.1	103 ± 16.4	691 ± 16.4	81.1	544
	1.5[b]	220[b]	–	147[b]	–
6	14.7 ± 3.4	8,951 ± 2,434	15,000 ± 2,526	609	1,017
7	41 ± 6.7	8,452 ± 2,220	21,300 ± 7,976	206	520
8	14.1 ± 4.1	2,280 ± 760	5,630 ± 1,747	162	399
9	19.1 ± 5.7	154 ± 33	10,980 ± 4,485	8.1	575
10	2.60 ± 0.5	2,273 ± 868	5,027 ± 1,978	864	1,911
	1.9[b]	6,700[b]	–	3,526[b]	–
13	36.8 ± 9.4	2,685 ± 910	116,000 ± 48,750	73	3,152
	11[b]	10,000[b]	–	909[b]	–
14	1.77 ± 0.4	537 ± 131	323 ± 127	303	182
17	3.01 ± 0.4	5,723 ± 1,660	6,928 ± 2,326	1901	2301
20	12.5 ± 3.0	20,390 ± 5,150	96,500 ± 34,050	1,622	7,677
22	26.4 ± 4.8	70,620 ± 15,050	134,600 ± 60,275	2,675	5,098

[a]Heterologously expressed human receptors were used. α4β2 and α3β4 nAChR subtypes were expressed in HEK293 cells; human α7 nAChR was expressed in SH-SY5Y human neuroblastoma cells. Binding was assessed with [^{3}H]epibatidine for α4β2 and α3β4 nAChR subtypes and [^{125}I]α-bungarotoxin for α7 subtype. K_i values (in nM) were derived from the average value of three independent competition binding experiments for each compound on each subtype.
[b]Binding data (K_i nM) based on α4β2 and α3β4 rat subtypes reported[32] for (−)-cytisine **1** and racemic ligands (±)-**10** and (±)-**13**; corresponding data for α7 nAChR subtype were not reported.

(α4β2, α3β4, and α7) for a series of C(10) ligands, all as single enantiomers, are presented in Table 1 together with values for (−)-cytisine **1** for comparison. Kozikowski and Kellar[32] have previously reported binding affinities for racemic 10-methyl and 10-(hydroxymethyl)cytisines ((±)-**10** and (±)-**13**, respectively), and their data using rat nAChR subtypes are included for comparison in Table 1. The modest differences in K_i values between the present study and that reported earlier can be accounted for by species (rat versus human) differences and/or their use of racemic ligands.

The data documented in Table 1 confirm that C(10)-substituted cytisine ligands have preferential binding affinity for α4β2 nAChR versus α3β4 or α7 nAChR. All C(10) ligands bind to α3β4 and α7 nAChR with a lower affinity than cytisine **1**, except 10-(perfluorophenyl)cytisine **9**, which has a similar affinity at α3β4 as **1**, and bromide **14**, which has a (modestly) higher affinity for α7 than does cytisine **1**. Moreover, binding affinities in the high nanomolar range are retained for the α4β2 nAChR subtype, such that bromide **14** and the 10-methyl and 10-ethyl derivatives **10** and **17** have affinities comparable with that of cytisine **1**.

Increasing the size of the C(10) alkyl substituent (using the ligand series outlined in Scheme 3) shows that although a small loss of potency at the α4β2 nAChR subtype is associated with the 10-isopropyl and 10-*tert*-butyl analogs **20** and **22**, these two ligands show markedly increased levels of selectivity (5,000- to 7,000-fold) against the α7 subtype.

Functional Assays

In the second set of biological experiments, we evaluated the series of C(10)-substituted ligands (**6–10**, **13**, **14**, **17**, **20**, and **22**) over the concentration range 1 nM to 100 μM for their functional potency and efficacy as agonists by determining their ability to activate currents in *Xenopus* oocytes heterologously expressing human α4β2, α3β4, or α7 nAChR subtypes (Figures 2A and 2B; Table S1). Acetylcholine
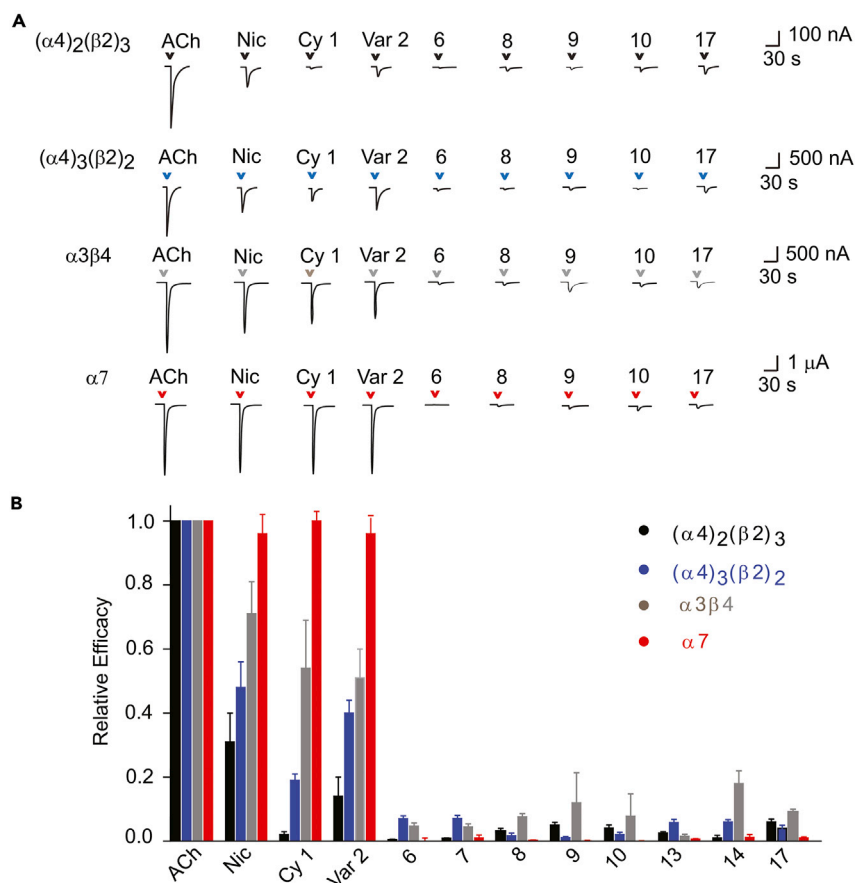
Figure 2. Functional Effects of C(10)-Substituted Cytisine Ligands on (α4)₂(β2)₃, (α4)₃(β2)₂, α3β4, and α7 nAChR Subtypes

Figure360▷ For a Figure360 author presentation of Figure 2, see http//dx.doi:10.1016/j.chempr.2018.05.007#mmc4.

(A) Representative traces of the current responses of (α4)₂(β2)₃, (α4)₃(β2)₂, α3β4, and α7 nAChR subtypes elicited by C(10)-substituted cytisine (Cy) ligands with the highest binding affinities for α4β2 nAChRs (6, 8, 9, 10, and 17) tested at 100 μM. Current responses were measured by two-electrode voltage-clamp recordings from *Xenopus* oocytes heterologously expressing (α4)₂(β2)₃ and (α4)₃(β2)₂ (the high and low acetylcholine [ACh] affinity stoichiometries, respectively), α3β4, or α7 nAChR subtypes, as detailed in the Supplemental Information. Current responses to 100 μM C(10) compounds were maximal responses for (α4)₂(β2)₃, (α4)₃(β2)₂, and α3β4 nAChR. Maximal current responses were elicited by 1 mM ACh, 100 μM nicotine (Nic), 100 μM Cy 1, and 100 μM varenicline 2 (Var) for comparison. α7 nAChR responses to C(10) ligands were submaximal when tested at 100 μM and less than 1% of the maximal ACh response (Table S1). Maximal current responses were elicited by 1 mM ACh, Nic, Cy 1, and Var 2. Arrowheads indicate compound application onto *Xenopus* oocytes expressing (α4)₂(β2)₃ (black), (α4)₃(β2)₂ (blue), α3β4 (gray), and α7 (red) nAChR.

(B) Relative efficacies of C(10)-substituted Cy ligands for activating (α4)₂(β2)₃, (α4)₃(β2)₂, α3β4, and α7 nAChR subtypes; comparison with ACh, Nic, Cy 1, and Var 2. Relative efficacy was determined with the following equation: (maximal response to test compound)/(maximal response to ACh) (1 mM). The C(10)-substituted ligands shown were tested over a concentration range of 1 nM to 100 μM, and maximal responses were achieved at 100 μM C(10)-substituted ligand for (α4)₂(β2)₃, (α4)₃(β2)₂, and α3β4 nAChR. At 100 μM, the compounds elicited submaximal current responses when applied to α7 nAChRs. Values are the mean ± SEM of six or seven independent experiments carried out on oocytes from five or six different *Xenopus* donors. Functional potencies (EC₅₀) were estimated for ligands with agonist efficacy greater than 0.1 by non-linear regression with GraphPad software and are shown in Table S1.

was assayed in parallel as a fully efficacious, non-selective agonist. Nicotine, cytisine 1, and varenicline 2 were also included for comparative purposes. We examined the two stoichiometries of the α4β2 nAChR by separately expressing the human receptors (α4)$_2$(β2)$_3$ (high sensitivity for acetylcholine and nicotine) and (α4)$_3$(β2)$_2$ (low sensitivity for acetylcholine and nicotine).[37]

The C(10) ligands behaved as partial agonists at (α4)$_2$(β2)$_3$ and (α4)$_3$(β2)$_2$ receptors and produced responses that were much smaller than those of acetylcholine but of similar magnitude to those currents produced by cytisine 1 (Figure 2A). Maximal responses were achieved by concentrations of 30–100 μM, indicating potency comparable with that of the parent cytisine 1. Our ligands also activated α3β4 nAChRs but with markedly lower efficacy than observed for cytisine 1. Consistent with their low binding affinities at α7 nAChR (Table 1), C(10) cytisine ligands applied over the same concentration range (1 nM–100 μM) showed negligible activity at α7 nAChR; at the highest concentration (100 μM), they either failed to induce any measurable current responses (6) or activated currents that were less than 1% of the maximal acetylcholine response (ligands 7–10, 13, 14, and 17 in Figure 2B; functional data relating to the alkyl series, including ligands 20 and 22, are shown in Figure S3).

When tested at higher concentrations (up to 3 mM), with the exception of ligand 6, which displayed no agonist activity at α7 nAChR, the C(10) ligands activated current responses with increased amplitudes (Table S1). For ligands 7, 9, 13, 20, and 22, the amplitudes of the responses were too low for constructing meaningful concentration-response curves. However, for compounds 8, 10, 14, and 17, it was possible to generate full concentration-response curves: the estimated efficacies for these ligands were 20%–40% of that of acetylcholine. Their potencies at α7 nAChR were in the mM range: 8, 1.55 ± 0.35 mM; 10, 1.60 ± 0.20 mM; 14, 1.58 ± 0.15 mM; 17, 1.70 ± 0.18 mM (Figure S2; Table S1). This is in marked contrast to the more than two orders of magnitude greater potency and full agonism of cytisine 1 and varenicline 2 at human (Figure 2), chick,[24] and rat[25] α7 nAChR.

Although the data shown in Figure 2 clearly demonstrate the partial agonist profiles of the C(10)-substituted cytisine variants at α4β2 nAChR, the limited agonist efficacy observed confounds accurate determination of their potency when the maximal current is less than 10% of that achieved by a full agonist like acetylcholine. As a result, we undertook further characterization of these C(10)-ligands at α4β2 nAChR to explore their partial agonism and obtain quantitative determinations of functional potency. We achieved this by assessing the ability of these ligands to act as competitive antagonists. This strategy is based on the rationale that a partial agonist fully occupies the agonist binding site while having low efficacy in activating the receptor: in occupying the binding site, a ligand will prevent other agonists from binding and activating the receptor; thus, in this circumstance, the partial agonist also acts as a partial competitive antagonist.[38] Indeed, this is the premise for the efficacy of varenicline as a smoking-cessation agent.[10] Where agonist efficacy is very low, as for the C(10)-substituted cytisines described here at nAChR subtypes, evaluation of the propensity of these ligands to act as competitive antagonists over a range of concentrations offers a more robust means of assessing their functional potency.[39] This is illustrated in Figure S1 for inhibition by cytisine 1 of acetylcholine-evoked responses of (α4)$_2$(β2)$_3$ and (α4)$_3$(β2)$_2$ nAChR. Note that the inhibition curve falls short of 100% inhibition, consistent with the partial agonist action of cytisine (magnified in the central panels of Figure S1). The inhibition curve allows determination of the concentration of cytisine 1, producing 50% inhibition
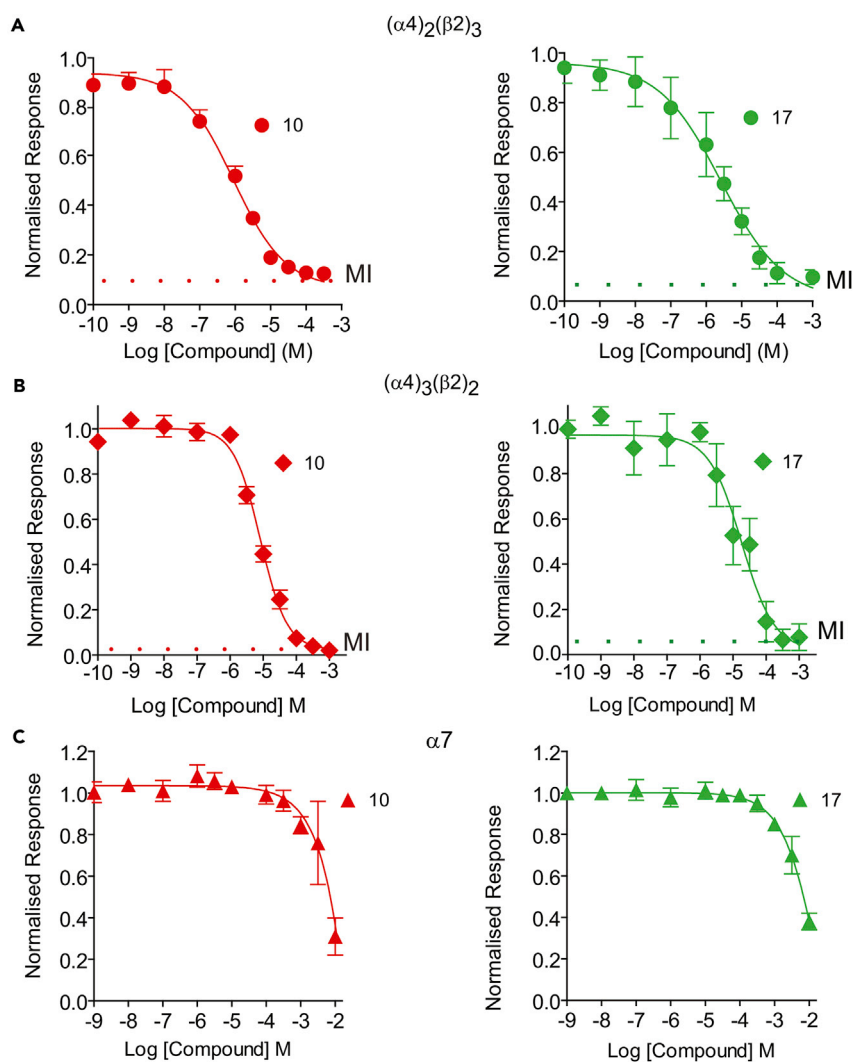
Figure 3. Competitive Antagonist Activity of C(10)-Substituted Cytisine Derivatives 10 and 17 on $(\alpha4)_2(\beta2)_3$, $(\alpha4)_3(\beta2)_2$, and $\alpha7$ nAChR Subtypes

The ability of ligands **10** and **17** to inhibit current responses elicited by ACh in *Xenopus* oocytes expressing $(\alpha4)_2(\beta2)_3$ (A), $(\alpha4)_3(\beta2)_2$ (B), and $\alpha7$ (C) nAChR subtypes was determined by two-electrode voltage-clamp recording as described in the Supplemental Information. Oocytes were stimulated with ACh at a concentration that produced 80% of its maximum response (EC_{80} concentration): 30 μM for $(\alpha4)_2(\beta2)_3$ (A) and 300 μM for $(\alpha4)_3(\beta2)_2$ (B) and $\alpha7$ (C) nAChR in the presence or absence of **10** or **17**, which were tested over a broad range of concentrations. Current responses in the presence of test ligand were compared with the control response to ACh alone (taken as 1.0) for construction of dose-response curves. Data points are the mean ± SEM from six independent determinations.

(half maximal inhibitory concentration [IC_{50}] 0.61 μM and 7.30 μM for $(\alpha4)_2(\beta2)_3$ and $(\alpha4)_3(\beta2)_2$ nAChR, respectively, Table S2). The latter value accords well with the directly estimated EC_{50} of 5.3 μM for activation of $(\alpha4)_3(\beta2)_2$ nAChR by cytisine **1** (Table S1), which validates this approach for assessing potency. The lower agonist efficacy of the $(\alpha4)_2(\beta2)_3$ nAChR subtypes precluded derivation of EC_{50} directly. Similarly, C(10)-substituted cytisine ligands inhibited acetylcholine-evoked responses of $(\alpha4)_2(\beta2)_3$ and $(\alpha4)_3(\beta2)_2$ nAChR expressed in *Xenopus* oocytes with residual activation that correlates with the directly determined agonist efficacy (Figures 3A and 3B; Table S2). In all cases, ligands were more potent inhibitors of the

$(\alpha 4)_2(\beta 2)_3$ stoichiometry. Consistent with the binding data (Table 1), the most potent inhibitors of $\alpha 4\beta 2$ nAChR were the 10-methyl and 10-ethyl cytisine derivatives **10** and **17**, which gave IC_{50} values (0.88 and 0.95 μM, respectively) comparable with that of cytisine **1** (IC_{50} 0.61 μM; Table S2).

We used the same approach to examine the ability of C(10)-substituted cytisine ligands **10** and **17** to inhibit acetylcholine-evoked responses from $\alpha 7$ nAChR (Figure 3C). This experiment clearly demonstrated that neither of these ligands has any antagonist activity at concentrations below 1 mM. This confirms that these ligands lack the ability to interact productively with $\alpha 7$ nAChR at sub-millimolar concentrations. This is consistent with the low-affinity binding constants shown in Table 1 and is in marked contrast to cytisine **1**. Given the series of alkyl derivatives associated with Scheme 3, this correlation between affinity (Table 1) and $\alpha 7$ function appears to extend to more sterically demanding substituents, such as those present in **20** and **22** (Figure S3). However, it would be premature to attribute (or indeed limit) this selectivity effect to substituent volume.

In summary, the C(10)-substituted cytisine ligands described in this paper retain the potent partial agonism of cytisine **1** at $\alpha 4\beta 2$ nAChR, regarded as a fundamental property for successful smoking-cessation agents.[10] These ligands display a preference for the $(\alpha 4)_2(\beta 2)_3$ receptor stoichiometry, and that discrimination can be attenuated by variation, for example, of the size of a C(10) alkyl substituent. In contrast to cytisine **1**, they lack the ability to activate (or inhibit) $\alpha 7$ nAChR at therapeutically meaningful concentrations, eliminating an interaction considered to be off-target for smoking cessation.[22,23] Furthermore, although these C(10) ligands are also weak partial agonists at $\alpha 3\beta 4$ nAChRs, observed efficacies at this subtype are consistently lower than those of cytisine **1** and varenicline **2** at $\alpha 3\beta 4$ nAChR.[25] Moreover, the binding affinities of $\alpha 3\beta 4$ nAChR for the C(10) compounds (with the exception of **9**) are markedly lower than that for cytisine **1**. As a consequence, these C(10)-substituted cytisine variants (exemplified by the C(10)-alkyl series **10**, **17**, **20**, and **22**) combine potent partial agonism with exceptional selectivity for $\alpha 4\beta 2$ nAChR, making them excellent lead candidates for further structural and pharmacological development.

Computational Docking Studies and Molecular Dynamics Simulations

Recognition of the opportunities associated with achieving a specific modification of cytisine at C(10) was guided by computational modeling of the mode of binding (and differences associated with that mode of binding) of a series of prototype ligands, namely cytisine **1** and the C(10) hydroxyl and C(10) methyl cytisine analogs **6** and **10**, respectively. We carried out this study by using appropriate crystallographic data[40,41] to derive human homology models in order to dock ligands into the binding sites of the three key nAChR subtypes: $\alpha 4\beta 2$, $\alpha 3\beta 4$, and $\alpha 7$. These models suggest three factors in the immediate environment of the agonist binding site to rationalize the enhanced $\alpha 4\beta 2$ receptor selectivity compared with that of $\alpha 3\beta 4$ and $\alpha 7$ nAChR for **1**, **6**, and **10** in terms of binding affinities. Although this study ultimately guided the selection of C(10) as the preferred site for modification, it also provides a framework for interpreting the selectivity for C(10)-substituted cytisine ligands presented in Table 1.

Ligands were docked into these three receptor subtypes in poses corresponding to those observed in the crystal structures of the acetylcholine binding protein (Ac-AChBP) (from *Aplysia californica*) with cytisine **1** and with varenicline **2** (PDB: 4BQT and PDB: 4AFT, respectively),[40] and the resulting complexes were relaxed by energy minimization. The Supplemental Information provides full
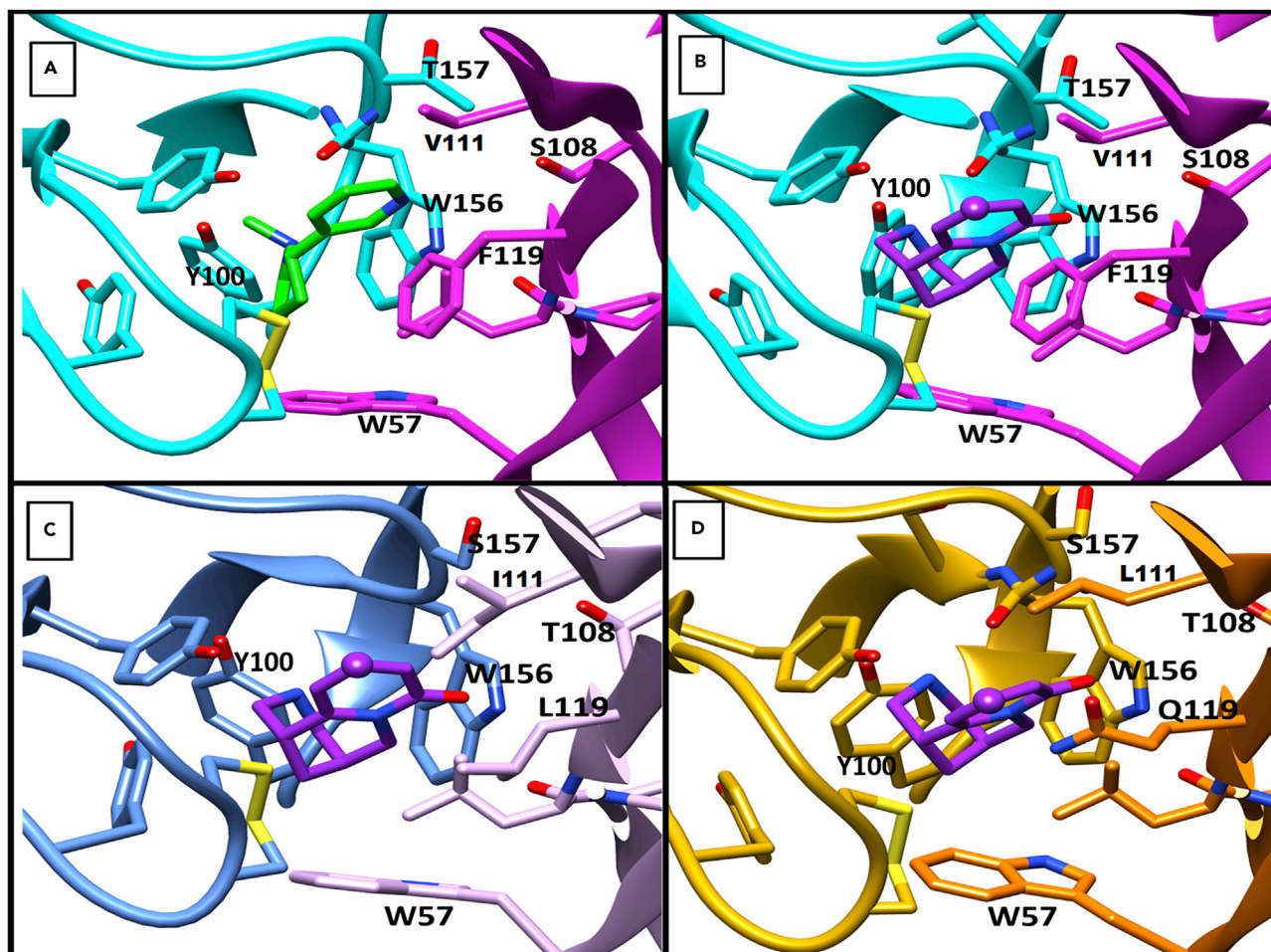
Figure 4. Binding-Site Orientations of Nicotine and Cytisine 1 in α4β2, α3β4, and α7 nAChR Subtypes

For clarity, all residue numbering refers to the analogous positions in the PDB: 5KXI crystal structure of the (α4)$_2$(β2)$_3$ nAChR with nicotine bound.[41] W57 is analogous to the TrpD referred to by Tavares et al.,[29] and W156 is analogous to TrpB. The solid sphere corresponds to the C(10) position within cytisine 1.

(A) The position of nicotine in the crystal structure of α4β2 PDB: 5KXI[41] (α subunit in cyan, β subunit in magenta, and nicotine in green).

(B) Cytisine 1 docked into the binding pocket of α4β2 (α subunit in cyan, β subunit in magenta, and cytisine 1 in purple); Video S1.

(C) Cytisine 1 docked into the model of human α3β4 (α subunit in blue, β subunit in mauve, and cytisine 1 in purple). Note the residues immediately lining the binding pocket: F119 (α4β2) is substituted by L119 (α3β4), and V111 (α4β2) is replaced by the bulkier I111 (α3β4). This modifies the hydrophobicity, shape, and space of the binding pocket. Also note the reversal of the positions of the (α4β2) S108 and T157 positions to T108 and S157 (α3β4), which may affect the hydrogen-bonding network around the cytisine carbonyl.

(D) Cytisine 1 docked into the model of the human α7 (one α subunit in yellow, neighboring α subunit in orange, and cytisine 1 in purple). This model illustrates that the substitutions include the same serine-threonine switch seen in α3β4; hydrophobic F119 is replaced by a more polar Q119, and V111 of α4β2 is also replaced with a bulkier leucine.

details together with an animation (Video S1) showing a view around the ligand binding site with cytisine docked into the α4β2 nAChR complex; key residues are labeled according to the recently reported human α4β2 nAChR crystal structure PDB: 5KXI and depict the desensitized, non-conducting conformation.[41] As expected, the modeled complexes of cytisine 1 and the corresponding C(10) variants share the core interactions observed in the Ac-AChBP-cytisine complex (PDB: 4BQT) and as described by Dougherty.[27,28] The protonated secondary amine N(3) binds with a combination of a cation-π interaction and hydrogen bonding within the α subunit.[29] Hydrogen bonds to the side chain of TyrA (Y100) and the amide carbonyl of TrpB (W156) are also present. (Where applicable, we adhere to the amino acid nomenclature and numbering scheme used by

Dougherty and co-workers.[27] For residues [subtype based] outside this scheme, numbering is according to positions within the crystal structure of the human α4β2 receptor [PDB: 5KXI].[41]) The pyridone carbonyl oxygen of cytisine **1** (and related C(10)-derivatives) is orientated toward the amide nitrogen and carbonyl of L121 within the protein backbone with space for bridging water molecules (as present in the crystal structure of varenicline with Ct-AChBP[42]), providing a hydrogen-bonding network with the side-chain hydroxyl of S108 (α4β2) or T108 (α3β4 and α7). The crystal structure of nicotine bound in the human α4β2 nAChR protein is shown in Figure 4A, and models of cytisine **1** bound to the three receptor subtypes (α4β2, α3β4, and α7) are shown in Figures 4B–4D, illustrating similar modes of ligand binding in each case. The C(10) position of cytisine **1** is highlighted by the solid purple sphere showing that a C(10) substituent will project into the aperture of the active site pocket enabling interactions with residues in the C loop or the neighboring subunit. For comparison, analogous models of varenicline **2** in all three receptor subtypes are shown in Figure S4, including a superposition of varenicline **2** and 10-methylcytisine **10** in the binding site of human α4β2 subtype.

In addition to performing docking studies, we carried out molecular dynamics (MD) simulations of the extracellular region of the α4β2, α3β4, and α7 nAChR subtype complexes with nicotine, cytisine **1**, and 10-methylcytisine **10** to better understand the molecular determinants that modulate ligand binding in these receptors. The ligands were placed into two of the nAChR binding pockets located at the subunit interfaces. The resulting complexes were relaxed by energy minimization and equilibrated, and MD simulations were performed for 100 ns without any restraints on the systems; see the Supplemental Information for full details and graphical outputs. A simple measure of the overall stability of the protein during the MD simulations can be obtained by plotting the root-mean-square deviation of the protein atoms with respect to their initial positions as a function of time. As can be observed in Figures S5–S8, there was little conformational drift in the overall protein structure during the simulation time in the nine simulations performed.

In all the nicotine and cytisine **1**-bound complexes, the ligand exhibited similar dynamic behavior such that it remained generally in the same binding orientation (within both binding pockets 1 and 2) throughout the simulation (Figures S9, S10, and S12). Furthermore, the two canonical interactions between nicotine and TrpB[27–29] were always present (Figures S13 and S14). In contrast, ligand dynamics were more diverse in the 10-methylcytisine **10** complexes (Figures S11 and S12); they showed higher mobility in the α7 subtype (mainly in binding pocket 2). This increased conformational variability could be associated with the lower α7 binding affinity (Table 1) and functional potency (Table S1) observed for 10-methylcytisine **10**.

In the α7 subtype, the ligand dynamics were modulated by the behavior of R81. During the simulation, the flexible side chain of R81 reoriented toward the binding pocket and moved close to the C(10) methyl of **10** (Video S2). This side-chain movement induced a change in the ligand binding mode, which resulted in the loss of interactions with TrpB (Figures S13 and S14).

DISCUSSION

This study exploited chemistry to generate a series of potent cytisine derivatives with enhanced selectivity for α4β2 nAChRs that facilitate an exploration of their molecular interactions with the nAChR agonist binding sites to provide a rational explanation of their selectivity profiles.

The first observation from the binding data in Table 1 is that 10-methylcytisine **10** binds with higher affinity than 10-hydroxycytisine **6** to each of the receptor subtypes and in line with the avidity ranking α4β2 > α3β4 > α7. This is consistent with our modeling, which suggests that binding of the less hydrophilic 10-methyl moiety (i.e., ligand **10**) is favored, as outlined next. The C(10) substituent on the cytisine scaffold is positioned within a hydrophobic region of the binding site in the β subunit. The hydrophobicity in this region is provided partly by the disulfide linkage in the α-chain C loop and a conserved leucine residue (β-chain L121) across these three nAChR subtypes. Furthermore, after comparing the homology models, residue 119 was also identified as potentially playing a key role in subtype discrimination. In the α4β2 subtype this residue is phenylalanine (F119), whereas the equivalent positions in the α3β4 and α7 are occupied by leucine and glutamine, respectively. This decrease in hydrophobicity[43,44] in the binding pocket of the α7 subtype could correlate with the lower binding affinity observed for **10**. Other key binding site residues with the potential to interact with a C(10) substituent are the hydroxyl of TyrC2 (Y204) and the amide carbonyl oxygen of T157. These residues could, in the case of 10-hydroxycytisine **6**, provide compensatory hydrogen-bonding interactions in an otherwise hydrophobic environment.

Secondly, modeling indicates that the α4β2, α3β4, and α7 nAChR subtypes differ in terms of the hydrophobic residue located at position 111 situated proximal to C(9) and C(10) of cytisine **1**: residue 111 is valine (in α4β2), isoleucine (in α3β4), and leucine (in α7). From this, we infer that bulkier residues (I111 and L111) in this region of the binding site serve to modulate the agonist binding cavity and are less accommodating of a more sterically demanding C(10)-substituted cytisine variant.

Our third observation is associated with the differences between receptor subtypes of the S108-T157 hydrogen-bond network in α4β2. Notably, the position of these residues is reversed in both α3β4 and α7, i.e., T108 and S157. This inversion might change not only the shape of the binding pocket but also the hydrogen bonds formed with the ligand.

Modeling of the three key nAChR subtype complexes allowed us to explore the wider binding region beyond the primary interactions already established for cytisine **1**. This work suggests several interactions specific to cytisine **1** in addition to those already characterized, some of which would be amenable to further investigation. These interactions (or some combination of them) might not only help to explain how cytisine **1** is differentiated from other nicotinic ligands but also suggest how a C(10) substituent could be exploited to modulate these differences and provide enhanced selectivity for α4β2 over both α3β4 and α7 nAChRs.

The relationship between cytisine **1**, varenicline **2**, and the C(10)-variants (e.g., **10**) reported here has been discussed (Figure S4) but raises the options associated with functionalization of varenicline **2**. Within the β subunit, this would involve targeting the quinoxaline moiety of **2**. This area of varenicline is amenable to C–H activation[45–49] (and other chemistry,[50] as are other parts of the scaffold[51]), and although quinoxaline-substituted derivatives have been reported, no corresponding biological details are available. One of the issues that does arise here and that has significant implications for any pharmacological assessment is that varenicline **2** is a *meso* compound. Monosubstitution within the quinoxaline unit breaks that symmetry, and although further substitution can resolve that issue, this complicates analysis of any resulting structure-activity relationship.

In conclusion, we have validated C(10) substitution of cytisine **1** as a viable mechanism for (1) eliciting increased selectivity for α4β2 versus α3β4 and, in particular, α7 nAChR subtypes; (2) retaining profound partial agonism at α4β2 nAChR; and (3) suppressing α7 agonism. We have solved the critical challenge of accessing this class of cytisine ligand by site-specific C–H functionalization of (−)-cytisine by using Ir-catalyzed borylation. This makes C(10)-substituted cytisine ligands available directly from the parent compound (i.e., **1**) in enantiomerically pure form, and the tractability associated with this chemistry opens up the range of structural variation that is accessible. We can now explore the structural determinants required for both binding and function to further refine nAChR subtype selectivity. In addition, given the relatively low lipophilicity of cytisine **1** compared with both nicotine and varenicline **2**,[22] the flexibility enabled by C–H activation chemistry provides an opportunity to identify new cytisine-based ligands for, e.g., smoking cessation, with improved penetration across the blood-brain barrier to achieve a more effective therapeutic benefit.

EXPERIMENTAL PROCEDURES

Full details of synthetic chemistry, receptor binding and functional studies, docking, and MD are provided in the Supplemental Information.

SUPPLEMENTAL INFORMATION

Supplemental Information includes Supplemental Experimental Procedures, 24 figures, 2 tables, and 2 videos and can be found with this article online at https://doi.org/10.1016/j.chempr.2018.05.007.

AUTHOR CONTRIBUTIONS

Conceptualization, H.R.C., R.B.S., A.J.M., S.W., and T.G.; Methodology, H.R.C. and A.H. (chemical synthesis), C.G., S.G.D.V., T.M.V., I.B., and S.W. (binding affinity and receptor function assays and interpretation), K.E.R., A.J.M., and R.B.S. (initial computational studies, parameters, and models), D.K.S. (subtype-specific homology models and insights into receptor differentiation), A.S.F.O., A.J.M., and R.B.S. (MD simulations and analysis); Writing – Original Draft, all authors; Writing – Review & Editing, H.R.C., R.B.S., A.J.M., D.K.S., A.S.F.O., I.B., S.W., and T.G.; Funding Acquisition, R.B.S., A.J.M., and T.G.; Supervision, R.B.S., A.J.M., I.B., and T.G.

DECLARATION OF INTERESTS

H.R.C. and T.G. are named inventors on a patent held by the University of Bristol. The patent has been licensed by the University of Bristol to Achieve Life Sciences. The University of Bristol and H.R.C. and T.G. are financial beneficiaries.

Chem

CellPress

REFERENCES AND NOTES

1. Gotti, C., Zoli, M., and Clementi, F. (2006). Brain nicotinic acetylcholine receptors: native subtypes and their relevance. Trends Pharmacol. Sci. 27, 482–491.

2. Albuquerque, E.X., Pereira, E.F.R., Alkondon, M., and Rogers, S.W. (2009). Mammalian nicotinic acetylcholine receptors: from structure to function. Physiol. Rev. 89, 73–120.

3. Taly, A., Corringer, P.J., Guedin, D., Lestage, P., and Changeux, J.P. (2009). Nicotinic receptors: allosteric transitions and therapeutic targets in the nervous system. Nat. Rev. Drug Discov. 8, 733–750.

4. Miwa, J.M., Freedman, R., and Lester, H.A. (2011). Neural systems governed by nicotinic acetylcholine receptors: emerging hypotheses. Neuron 70, 20–33.

5. Posadas, I., Lopez-Hernandez, B., and Cena, V. (2013). Nicotinic receptors in neurodegeneration. Curr. Neuropharmacol. 11, 298–314.

6. Lewis, A.S., Mineur, Y.S., Smith, P.H., Cahuzac, E.L.M., and Picciotto, M.R. (2015). Modulation of aggressive behavior in mice by nicotinic receptor subtypes. Biochem. Pharmacol. 97, 488–497.

7. Mathers, C.D., and Loncar, D. (2006). Projections of global mortality and burden of disease from 2002 to 2030. PLoS Med. 3, e442.

8. Jha, P. (2015). Deaths and taxes: stronger global tobacco control by 2025. Lancet 385, 918–920.

9. Conference of the Parties to the WHO FCTC. (2003). WHO Framework Convention on Tobacco Control (World Health Organization).

10. Rollema, H., Coe, J.W., Chambers, L.K., Hurst, R.S., Stahl, S.M., and Williams, K.E. (2007). Rationale, pharmacology and clinical efficacy of partial agonists of alpha(4)beta(2) nACh receptors for smoking cessation. Trends Pharmacol. Sci. 28, 316–325.

11. Syed, B.A., and Chaudhari, K. (2013). Smoking cessation drugs market. Nat. Rev. Drug Discov. 12, 97–98.

12. Lloyd, G.K., and Williams, M. (2000). Neuronal nicotinic acetylcholine receptors as novel drug targets. J. Pharmacol. Exp. Ther. 292, 461–467.

13. Jensen, A.A., Frolund, B., Lijefors, T., and Krogsgaard-Larsen, P. (2005). Neuronal nicotinic acetylcholine receptors: structural revelations, target identifications, and therapeutic inspirations. J. Med. Chem. 48, 4705–4745.

14. Rouden, J., Lasne, M.C., Blanchet, J., and Baudoux, J. (2014). (-)-Cytisine and derivatives: synthesis, reactivity, and applications. Chem. Rev. 114, 712–778.

15. Etter, J.F. (2006). Cytisine for smoking cessation - a literature review and a meta-analysis. Arch. Intern. Med. 166, 1553–1559.

16. Etter, J.F., Lukas, R.J., Benowitz, N.L., West, R., and Dresler, C.M. (2008). Cytisine for smoking cessation: a research agenda. Drug Alcohol Depend. 92, 3–8.

17. Walker, N., Howe, C., Glover, M., McRobbie, H., Barnes, J., Nosa, V., Parag, V., Bassett, B., and Bullen, C. (2014). Cytisine versus nicotine for smoking cessation. N. Engl. J. Med. 371, 2353–2362.

18. West, R., Zatonski, W., Cedzynska, M., Lewandowska, D., Pazik, J., Aveyard, P., and Stapleton, J. (2011). Placebo-controlled trial of cytisine for smoking cessation. N. Engl. J. Med. 365, 1193–1200.

19. Cahill, K., Lindson-Hawley, N., Thomas, K.H., Fanshawe, T.R., and Lancaster, T. (2016). Nicotine receptor partial agonists for smoking cessation. Cochrane Database Syst. Rev. https://doi.org/10.1002/14651858.CD006103.pub7.

20. Coe, J.W., Brooks, P.R., Vetelino, M.G., Wirtz, M.C., Arnold, E.P., Huang, J.H., Sands, S.B., Davis, T.I., Lebel, L.A., Fox, C.B., et al. (2005). Varenicline: an alpha 4 beta 2 nicotinic receptor partial agonist for smoking cessation. J. Med. Chem. 48, 3474–3477.

21. Coe, J.W., Rollema, H., and O'Neill, B.T. (2009). Case history: Chantix (TM)/Champix (TM) (varenicline tartrate), a nicotinic acetylcholine receptor partial agonist as a smoking cessation aid. Annu. Rep. Med. Chem. 44, 71–101.

22. Rollema, H., Chambers, L.K., Coe, J.W., Glowa, J., Hurst, R.S., Lebel, L.A., Lu, Y., Mansbach, R.S., Mather, R.J., Rovetti, C.C., et al. (2007). Pharmacological profile of the alpha(4)beta(2) nicotinic acetylcholine receptor partial agonist varenicline, an effective smoking cessation aid. Neuropharmacology 52, 985–994.

23. Rollema, H., Shrikhande, A., Ward, K.M., Coe, J.W., Tseng, E., Wang, E.Q., De Vries, M., Cremers, T., Bertrand, S., and Bertrand, D. (2009). Preclinical properties of the alpha 4 beta 2 nAChR partial agonists varenicline, cytisine and dianicline translate to clinical efficacy for nicotine dependence. Biochem. Pharmacol. 78, 918–919.

24. Amar, M., Thomas, P., Johnson, C., Lunt, G.G., and Wonnacott, S. (1993). Agonist pharmacology of the neuronal alpha-7 nicotinic receptor expressed in Xenopus-oocytes. FEBS Lett. 327, 284–288.

25. Mihalak, K.B., Carroll, F.I., and Luetje, C.W. (2006). Varenicline is a partial agonist at alpha 4 beta 2 and a full agonist at alpha 7 neuronal nicotinic receptors. Mol. Pharmacol. 70, 801–805.

26. Peng, C., Stokes, C., Mineur, Y.S., Picciotto, M.R., Tian, C.J., Eibl, C., Tomassoli, I., Guendisch, D., and Papke, R.L. (2013). Differential modulation of brain nicotinic acetylcholine receptor function by cytisine, varenicline, and two novel bispidine compounds: emergent properties of a hybrid molecule. J. Pharmacol. Exp. Ther. 347, 424–437.

27. Van Arnam, E.B., and Dougherty, D.A. (2014). Functional probes of drug receptor interactions implicated by structural studies: cys-loop receptors provide a fertile testing ground. J. Med. Chem. 57, 6289–6300.

28. Dougherty, D.A. (2008). Cys-loop neuroreceptors: structure to the rescue? Chem. Rev. 108, 1642–1653.

29. Tavares, X.D.S., Blum, A.P., Nakamura, D.T., Puskar, N.L., Shanata, J.A.P., Lester, H.A., and Dougherty, D.A. (2012). Variations in binding among several agonists at two stoichiometries of the neuronal, alpha 4 beta 2 nicotinic receptor. J. Am. Chem. Soc. 134, 11474–11480.

30. Yohannes, D., Procko, K., Lebel, L.A., Fox, C.B., and O'Neill, B.T. (2008). Deconstructing cytisine: the syntheses of (+/-)-cyfusine and (+/-)-cyclopropylcyfusine, fused ring analogs of cytisine. Bioorg. Med. Chem. Lett. 18, 2316–2319.

31. Chellappan, S.K., Xiao, Y.X., Tueckmantel, W., Kellar, K.J., and Kozikowski, A.P. (2006). Synthesis and pharmacological evaluation of novel 9- and 10-substituted cytisine derivatives. Nicotinic ligands of enhanced subtype selectivity. J. Med. Chem. 49, 2673–2676.

32. Kozikowski, A.P., Chellappan, S.K., Xiao, Y.X., Bajjuri, K.M., Yuan, H.B., Kellar, K.J., and Petukhov, P.A. (2007). Chemical medicine: novel 10-substituted cytisine derivatives with increased selectivity for alpha 4 beta 2 nicotinic acetylcholine receptors. ChemMedChem. 2, 1157–1161.

33. Durkin, P., Magrone, P., Matthews, S., Dallanoce, C., and Gallagher, T. (2010). Lactam enolate-pyridone addition: synthesis of 4-halocytisines. Synlett, 2789–2791.

34. Gray, D., and Gallagher, T. (2006). A flexible strategy for tri- and tetracyclic lupin alkaloids. synthesis of (+)-cytisine, (±)-anagyrine and (±)-thermopsine. Angew. Chem. Int. Ed. 45, 2419–2423.

35. Miura, W., Hirano, K., and Miura, M. (2017). Iridium-catalyzed site-selective C-H borylation of 2-pyridones. Synthesis 49, 4745–4752.

36. Hintermann, L., Xiao, L., and Labonne, A. (2008). A general and selective copper-catalyzed cross-coupling of tertiary Grignard reagents with azacyclic electrophiles. Angew. Chem. Int. Ed. 47, 8246–8250.

37. Moroni, M., Zwart, R., Sher, E., Cassels, B.K., and Bermudez, I. (2006). Alpha 4 beta 2 nicotinic receptors with high and low acetylcholine sensitivity: pharmacology, stoichiometry, and sensitivity to long-term exposure to nicotine. Mol. Pharmacol. 70, 755–768.

38. Papke, R.L., and Heinemann, S.F. (1994). Partial agonist properties of cytisine on neuronal nicotinic receptors containing the beta 2 subunit. Mol. Pharmacol. 45, 142–149.

39. Sharples, C.G.V., Kaiser, S., Soliakov, L., Marks, M.J., Collins, A.C., Washburn, M., Wright, E., Spencer, J.A., Gallagher, T., Whiteaker, P., and Wonnacott, S. (2000). UB-165: a novel nicotinic agonist with subtype selectivity implicates the alpha 4 beta 2* subtype in the modulation of dopamine release from rat striatal synaptosomes. J. Neurosci. 20, 2783–2791.

40. Rucktooa, P., Haseler, C.A., van Elk, R., Smit, A.B., Gallagher, T., and Sixma, T.K. (2012). Structural characterization of binding mode of smoking cessation drugs to nicotinic acetylcholine receptors through study of ligand complexes with acetylcholine-binding protein. J. Biol. Chem. _287_, 23283–23293.

41. Morales-Perez, C.L., Noviello, C.M., and Hibbs, R.E. (2016). X-ray structure of the human alpha 4 beta 2 nicotinic receptor. Nature _538_, 411–415.

42. Billen, B., Spurny, R., Brams, M., van Elk, R., Valera-Kummer, S., Yakel, J.L., Voets, T., Bertrand, D., Smit, A.B., and Ulens, C. (2012). Molecular actions of smoking cessation drugs at alpha 4 beta 2 nicotinic receptors defined in crystal structures of a homologous binding protein. Proc. Natl. Acad. Sci. USA _109_, 9173–9178.

43. Kyte, J., and Doolittle, R.F. (1982). A simple method for displaying the hydropathic character of a protein. J. Mol. Biol. _157_, 105–132.

44. Rose, G.D., Geselowitz, A.R., Lesser, G.J., Lee, R.H., and Zehfus, M.H. (1985). Hydrophobicity of amino-acid residues in globular proteins. Science _229_, 834–838.

45. Ji, Y.N., Brueckl, T., Baxter, R.D., Fujiwara, Y., Seiple, I.B., Su, S., Blackmond, D.G., and Baran, P.S. (2011). Innate C-H trifluoromethylation of heterocycles. Proc. Natl. Acad. Sci. USA _108_, 14411–14415.

46. Zhou, Q.H., Gui, J.H., Pan, C.M., Albone, E., Cheng, X., Suh, E.M., Grasso, L., Ishihara, Y., and Baran, P.S. (2013). Bioconjugation by native chemical tagging of C-H bonds. J. Am. Chem. Soc. _135_, 12994–12997.

47. Fujiwara, Y., Dixon, J.A., Rodriguez, R.A., Baxter, R.D., Dixon, D.D., Collins, M.R., Blackmond, D.G., and Baran, P.S. (2012). A new reagent for direct difluoromethylation. J. Am. Chem. Soc. _134_, 1494–1497.

48. Huff, C.A., Cohen, R.D., Dykstra, K.D., Streckfuss, E., DiRocco, D.A., and Krska, S.W. (2016). Photoredox-catalyzed hydroxymethylation of heteroaromatic bases. J. Org. Chem. _81_, 6980–6987.

49. Nuhant, P., Oderinde, M.S., Genovino, J., Juneau, A., Gagne, Y., Allais, C., Chinigo, G.M., Choi, C., Sach, N.W., Bernier, L., et al. (2017). Visible-light-initiated manganese catalysis for C-H alkylation of heteroarenes: applications and mechanistic studies. Angew. Chem. Int. Ed. _56_, 15309–15313.

50. Markovic, T., Rocke, B.N., Blakemore, D.C., Mascitti, V., and Willis, M.C. (2017). Pyridine sulfinates as general nucleophilic coupling partners in palladium-catalyzed cross-coupling reactions with aryl halides. Chem. Sci. _8_, 4437–4442.

51. Topczewski, J.J., Cabrera, P.J., Saper, N.I., and Sanford, M.S. (2016). Palladium-catalysed transannular C-H functionalization of alicyclic amines. Nature _531_, 220–224.